RSC Advances

ROYAL SOCIETY OF CHEMISTRY

www.rsc.org/advances

Journal Name

ARTICLE

One-step preparation of graphene oxide-poly(3,4 ethylenedioxythiophene) composite films for nonvolatile rewritable memory

Received 00th January 20xx,
Accepted 00th January 20xx

DOI: 10.1039/x0xx00000x

www.rsc.org/

Yongming Li and Xiuyuan Ni *

Nonvolatile rewritable memory devices were fabricated from the composite films of poly(3,4-ethylenedioxythiophene) (PEDOT) grown on graphene oxide (GO) substrate. A photopolymerization which used GO as the reaction initiator had been carried out for preparing the GO-PEDOT composite films of bilayer structure. The composite films were analyzed by specular reflection infrared spectroscopy, Raman, atomic force microscopy, field-emission scanning electron microscope coupled with energy-dispersive X-ray analysis and thermogravimetric analysis. The electronic properties of the as-prepared GO-PEDOT composite films were revealed by solid-phase ultraviolet photoelectron spectroscopy and X-ray photoelectron spectroscopy. Fabricated from the composite films, the ITO/GO-PEDOT/Al device exhibits the nonvolatile rewritable memory of high performance with the ON/OFF current ratio of 3×10^4 and turn-on voltage of 1.5 V. The current-voltage characteristics and resistance-temperature dependence at different resistance levels are discussed. The resistance of OFF state presents negative temperature dependence, indicating a typical semiconductor property. The resistance of ON state is found to increase with increasing temperature, indicating a metallic behavior.

Introduction

Resistance random access memory (RRAM) devices, which are based on the switching behavior of electrical conductivity, promise to provide the nonvolatile-memory information storage with the advanced properties.[1-5] Compared with the traditional charge-based memory devices such as the floating-gate nonvolatile semiconductor memory, RRAM devices show high density, rapid write-read speed, and low power consumption.[6,7] Among the various kinds of materials which have been used in the RRAM devices, the conductive polymers have attracted much attention due to easy processing, good environmental stability, and low cost.[8,9] The use of the polymers also opens the possibility of achieving flexible RRAM film devices, which promise to have broad applications.[10-13] Integrating conductive polymers with graphene materials has been recently explored with the aim of reaching favorite synergetic effects from the two materials. The majority of these studies intended to pursue the composites containing GO, which is decorated by the oxygen-contained groups (i.e. hydroxyl, epoxy and carboxyl) at the surface of the carbon planes.[14,15] The oxygen-contained groups provide the reactive sites for functionalizing GO to have the high solubility in organic solvents, differing from the heavy aggregation of graphene due to Van der Waals forces between the nanosheets.[14] The high solubility makes to convenient solution-technologies applicable to device preparation. It is also important that properly functionalizing groups has connected GO to the conductive polymers. In the memory devices of the GO-conductive polymer composites, the interface between the two components is one of the factors influencing nonvolatile-memory properties. An intimate interface has been regarded to promote both electron transfer and the stability of the devices.[16]

Several methods have been developed for preparing the GO-conductive polymer composites for RRAM devices. The carboxylic acid groups at the surface of GO have been usually chosen as the reaction sites. An efficient method was that the carboxylic acid reacted with diisocyanate compounds, giving rise to the amidation of GO.[8,17] The amine-containing GO had high solubility in organic solvents and good compatibility with the polymers. For example, Liu *et al* have grafted PVK to GO through the reaction of diisocyanate-modified GO with the carboxyl-terminated poly(N-vinylcarbazole)(PVK).[17,18] Another method was acyl chlorination of the carboxylic acid groups at GO, followed by the graft reaction of polymers with the acyl chloride moieties.[9,14,19] Zhuang *et al* connected the acyl chlorided GO to an arylamine-contained conductive polymer.[14] Moreover, Li *et al* have reported the atom transfer radical polymerization for the covalent graft of poly(tert-butyl acrylate) to GO nanosheets, and the grafted polymer brushes could enhance the solubility of GO in organic solvents.[20] The uniform and stable dispersion was obtained when the modified GO was mixed with poly(3-hexylthiophene) in toluene solvent.[21] By using the solution technologies such as

State Key Laboratory of Molecular Engineering of Polymers, Department of Macromolecular Science, Fudan University, Shanghai, 200433, The People's Republic of China. E-mail: xyni@fudan.edu.cn; Tel: +86-21-65640982; Fax: +86-21-65640293

spin coating, the active layers of the memory devices have been fabricated from these composite materials. In our previous work, we have reported a straightforward, one-step method to prepare the composite films of polypyrrole (PPy) and GO by using in suit photopolymerization.[16] Having realized the fact that GO is in nature of semiconductor and shows the photocatalytic ability, we used the photoexcitated GO to successfully initiate the polymerization of pyrrole. The results showed that the as-synthesized PPy strongly interacted with the GO substrate serving as the initiator, and the composite films devices exhibited the RRAM properties.[16] Moreover, the reaction mechanism of the photopolymerization has been correlated to the oxidization reactions at the surface of oxide semiconductors.[22]

PEDOT, one of important conjugated polymers,[23] has good chemical stability.[24] Both electrodeposition and oxidization polymerization have been used for preparing the binary composites consisting of PEDOT and the functionalized GO. In the electropolymerization, the polymerization of EDOT monomers was carried out in the presence of GO serving as the weak electrolyte.[25] As for the method of oxidization polymerization, the oxidizing agents such as $FeCl_3$ and $(NH_4)_2S_2O_8$) were added to the GO dispersion, followed by mixing the dispersion with an EDOT solution.[26,27] As reported, the as-prepared GO-PEDOT composites have been recently used for preparing supercapacitors and sensors.[25-27] It is mentioned that a memory device was prepared by blending poly(3,4-ethylenedioxythiophene):poly(styrenesulfonate) (PEDOT:PSS) with the reduced graphene oxide (rGO), and the ON/OFF current ratio was about 2 at 0.3V.[28] In this study, we obtain GO-PEDOT composite films by using the GO-initiated photopolymerization, and the new film devices which are fabricated from the GO-PEDOT composite films are found to show excellent RRAM properties. Distinguished from the electrodeposition and oxidization polymerization mentioned above, the GO-initiated photopolymerization here generates the novel bilayer film with PEDOT growing on the GO substrate. It is measured that the GO-PEDOT bilayer film devices exhibit the bistable electrical switching and nonvolatile rewritable memory with ON/OFF ratio as high as 3×10^4. Furthermore, the current-voltage characteristics and resistance-temperature dependence at different resistance levels are investigated with the aim of putting insight into the physical nature of resistance switching effects and mechanism of the charge conduction in the composite film devices.

Experimental

Materials

3,4-Ethylenedioxythiophene (EDOT) monomer (J&K Co., Ltd) was distilled under vacuum before use. GO was purchased from Nanjing XFNANO Materials Tech Co., Ltd and used as received. The Indium tin oxide (ITO) substrates (10 ohm/sheet, Shenzhen Nanbo Display Device Co., Ltd) were carefully cleaned and dried with nitrogen before use. The other materials of reagent grade were purchased from Sinopharm Chemical Reagent Co., Ltd and used as received.

Preparation of ITO/GO-PEDOT/Al memory device

Preparation of GO-PEDOT composite films. 0.5 g of methanol and 1.5 g of deionized water were mixed with 1 mg of GO. Subsequently, the bath ultrasonication was conducted for 3 h at the power of 140 W to obtain a uniform suspension. 20 drops of the as-obtained GO solution were spun onto ITO substrate at an angular speed of 1000 rpm. The substrates were dried in the air. One piece of GO substrate was placed upright in a quartz-glass reactor that was equipped with a water jacket connected to a circulator of $CuSO_4$ saturated solution, which was used as the light filter.[22] 0.01 mol of EDOT and 80 mL of deionized water were added to the reactor. The resulting mixture was stirred for 3 h under a nitrogen atmosphere. Then the reactor was subjected to UV irradiation at 365 nm for 3 h. The as-prepared GO-PEDOT hybrid film was rinsed with ethanol and then dried by nitrogen flow.

Fabrication of ITO/GO-PEDOT/Al Memory devices. The ITO/GO-PEDOT/Al memory devices were obtained by depositing Al electrode on the GO-PEDOT composite films grown on ITO. The Al top electrodes (0.5×0.5 mm^2 in size) were thermally evaporated through the shadow mask at a pressure of 10^{-7} Torr and a uniform depositing rate of 20 Å/s.

Measurement

Atomic Force Microscopy (AFM) was carried out by using a Multimode 8 instrument. Fourier transform infrared (FTIR) spectra were recorded on a Nicolet 6700 spectrometer using the specular reflectance technique. Raman spectra were measured by using an XploRA microscopic confocal Raman spectrometer employing a 532 nm laser beam. Field-emission scanning electron microscope coupling with energy-dispersive X-ray analysis (FESEM-EDX) was carried out with an Oxford Instrument X-MAX 50 at long-time acquisition. Thermogravimetric analysis (TGA) was performed in a PerkinElmer Pyris 1 TGA instrument at a heating rate of 20 °C min^{-1} under the nitrogen atmosphere. X-ray photoelectron spectroscopy (XPS) was carried out with a PHI-5000CESCA system (Perkin-Elmer) using Al Kα radiation. Solid-phase ultraviolet photoelectron spectroscopy (UPS) was conducted with a Thermo ESCALAB 250 spectrometer using HeI light (21.21 eV). The current-voltage and resistive switching characteristics of the fabricated RRAM devices were measured by using an Agilent B1500A semiconductor parameter analyzer under ambient conditions. Both of the electrical pulse and the bias voltage were applied to the top electrode Al. Meanwhile, the bottom electrode ITO was grounded.

Results and discussion

The structures of the composite films of PEDOT grown on the GO substrate

As indicated by the AFM images in Fig. 1, the GO materials which are used here consist of the flakes in the lateral dimensions around 2~5 μm. It is determined by 3D image that the thickness of GO is 0.9 nm (See inset in Fig. 1a). The GO

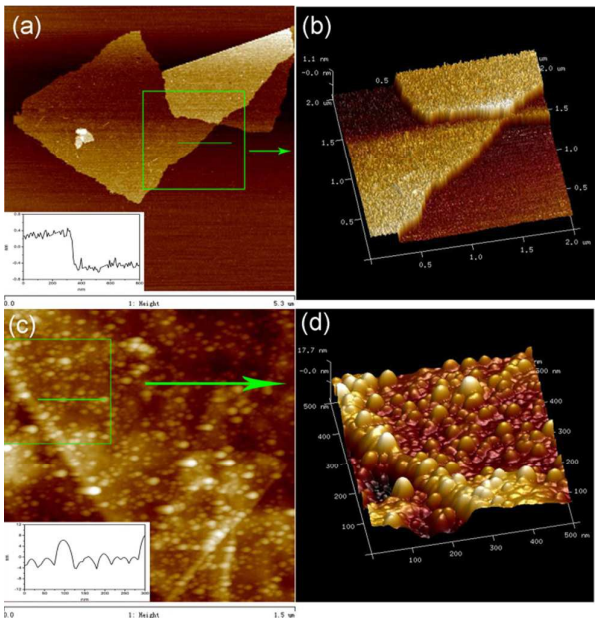

Fig. 1 The AFM 2D height images of (a) GO and (c) GO-PEDOT composite films, and AFM 3D height images of (b) GO and (d) GO-PEDOT composite films. Insets show the height profiles which are taken along the green lines in (a) and (c), respectively.

films were used as the photo-initiators by immersing GO substrate in the aqueous EDOT solution under the UV irradiation at the wavelength of 365 nm, as described in Experimental section. The typical morphologies of the reacted film are presented in Fig. 1c and Fig. 1d. It is found that as a result of the photochemical polymerization, the globular particles in sizes of about 50 nm homogeneously grown on the GO sheets (See inset in Fig. 1c). Fig. 2 shows the specular reflection infrared spectra measured from the GO, PEDOT and GO-PEDOT composite film, respectively. On comparison, the spectrum of GO-PEDOT composite film includes the characteristic absorption from both PEDOT and GO components. The three peaks at 690 cm^{-1}, 838 cm^{-1} and 983 cm^{-1} are attributed to the deformation modes of C-S-C in the

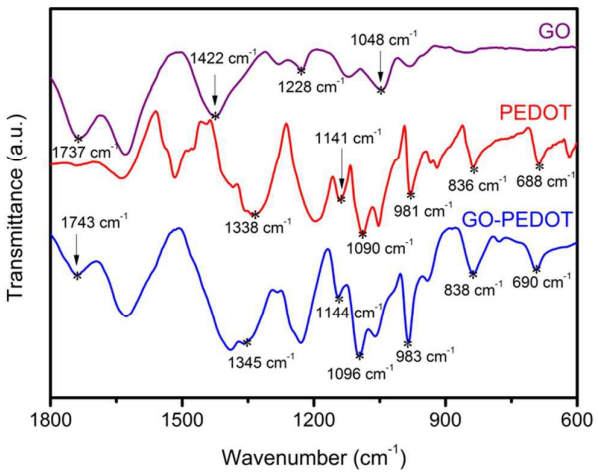

Fig. 2 The specular reflection infrared spectra measured from the GO, PEDOT and GO-PEDOT composite films.

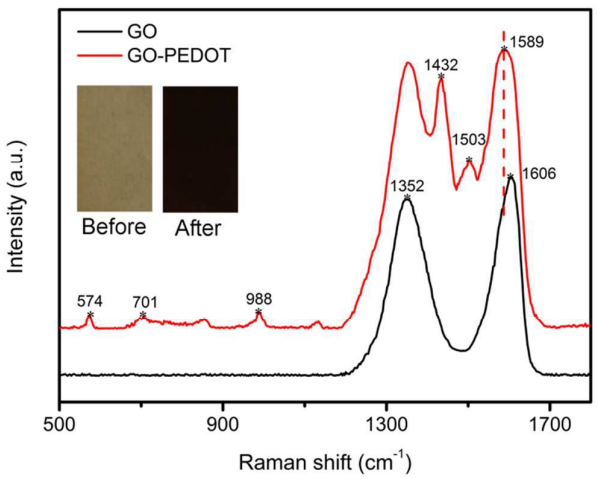

Fig. 3 The Raman spectra measured from the GO and GO-PEDOT composite films, respectively. The inset photographs represent the GO substrate before and after the photochemical reaction, respectively.

thiophene ring of PEDOT.[29] Both of the two peaks at 1096 cm^{-1} and 1144 cm^{-1} are ascribed to the C-O-C bending vibration of the ethylenedioxy moiety.[29] The peak at 1353 cm^{-1} is assigned to C-C stretching of the quinoidal structure of PEDOT.[29] These results prove that the globular nanoparticles of PEDOT have grown on the GO substrate.

Fig. 3 shows the Raman spectra measured from and GO-PEDOT composite film and the neat GO, respectively. In the spectrum of the GO-PEDOT composite film, the bands at 1503 cm^{-1} and 1432 cm^{-1} are attributed to C=C stretching of PEDOT.[29] The bands at 988 $cm^{-1}$and 574 cm^{-1} are assigned to the oxyethylene ring deformation.[29] The band at 701 cm^{-1} is ascribed to C-S-C symmetric deformation of the thiophene ring at PEDOT.[29] The results confirm the synthesis of PEDOT. In the GO spectrum, the two bands at 1352 cm^{-1} and 1606 cm^{-1} are attributed to the D-band and G-band, respectively.[27] The D-band arises from sp^3 C atoms, which is attributed to local defects and disorders.[27] The G-band is correlated to the vibration of sp^2-bonded carbon atoms in a 2-D hexagonal

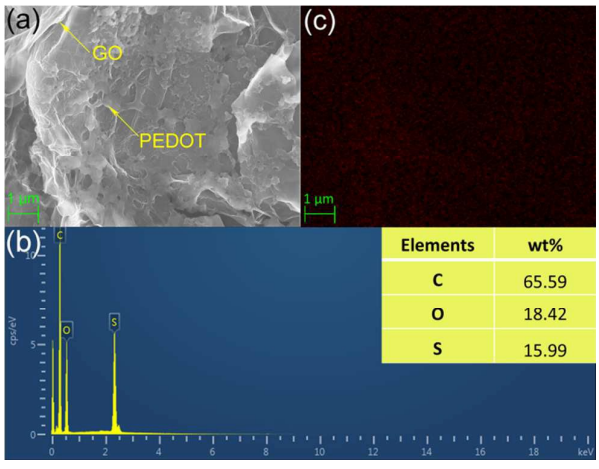

Fig. 4 (a) The FESEM photograph of the GO-PEDOT composites. (b) The EDX spectrum measured from the GO-PEDOT. (c) S elemental mapping of the GO-PEDOT composites.

lattice.[27] It is observed that as compared with the neat GO, the G band of the GO-PEDOT composite film shifts to lower wavelength significantly by 17 cm^{-1}. The result suggests that the GO substrate is interacted with the PEDOT layer.[16] As shown by the inset in Fig. 3, the PEDOT component has turned GO substrate dark.

FESEM-EDX was carried out to analyze the element distribution in the composite materials. Fig. 4 shows the FESEM photograph, EDX spectrum and sulfur elemental mapping of the GO-PEDOT composites. The EDX spectrum presents the signals of C, O and S elements, confirming the synthesis of PEDOT. According to the molecular formula of PEDOT and the EDX result that the content of S element is 16 % in the composites, we obtain that the content of PEDOT component is about 71 %. Moreover, the elemental mapping indicates that the S element of PEDOT is uniformly distributed. Fig. 5 shows the TGA curves of GO and GO-PEDOT samples under the nitrogen atmosphere at a rate of 20 °C·min^{-1}. It can be seen that GO shows a noteworthy mass loss in the temperatures ranging from 200 °C to 320 °C due to the decomposition of oxygen-containing groups.[30] At the temperatures ranging from 300 °C to 800 °C, the GO-PEDOT composites have larger weight-loss than the pure GO as the result of the PEDOT decomposition.[31] According to the final char yield of 28 % for the pure PEDOT,[31] we calculate that the content of PEDOT component in the GO-PEDOT is about 68 %, consistent with the result of EDX.

Fig. 6a shows the XPS survey spectrum measured from the GO-PEDOT composite films. The survey spectrum signals reveal the presence of C, O and S elements, agreeing with EDX spectrum as described above. Fig. 6b shows the C 1s core level spectrum of the composite films. Compared with the C 1s spectrum of the pristine GO, the C 1s spectrum of GO-PEDOT composite films has changed dramatically (See inset in Fig. 6b). By using the standard line-shape analysis, the C 1s spectrum is fitted with four components at 284.6 eV, 285.9 eV, 286.6 eV and 288.7 eV, respectively. The peak at 284.6 eV is assigned to the C-C/C=C. The peak at 285.9 eV is attributed to the C-S bond of PEDOT. The peaks at 286.6 eV and 288.7 eV are assigned to

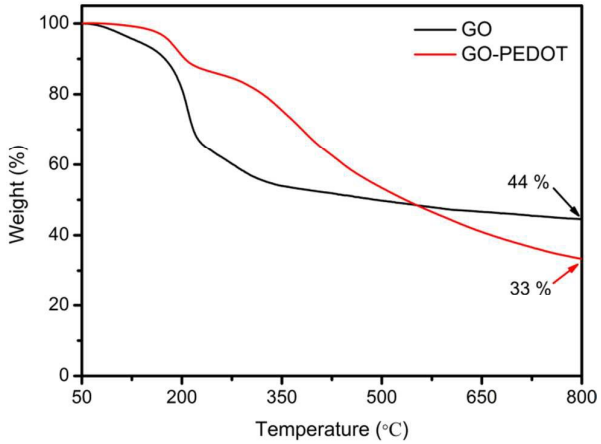

Fig. 5 The TGA curves of the pristine GO and the GO-PEDOT composites under nitrogen atmosphere.

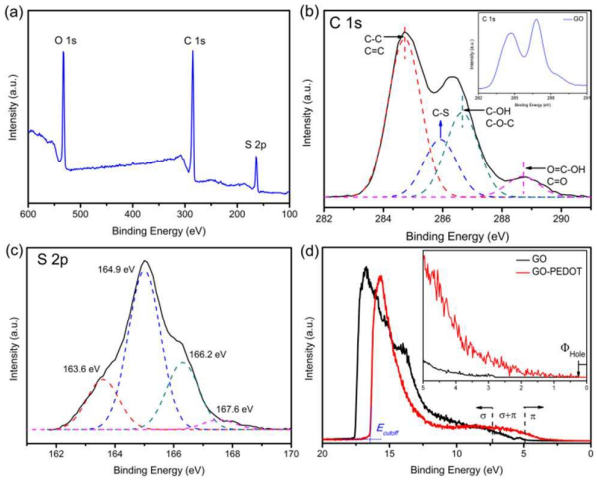

Fig. 6 The XPS spectra of GO-PEDOT composite films: (a) survey spectrum; (b) C1s; (c) S2p. Inset in (b) presents the C1s XPS spectrum of the pristine GO film. (d) The UPS spectra measured from the GO-PEDOT composite film and the neat GO films. Inset in (d) presents the UPS spectra for the GO-PEDOT composite film and the neat GO films on the low-energy side, respectively.

C-O and C=O, respectively.[32,33] As indicated by the high resolution XPS spectrum of S 2p in Fig. 6c, the peaks at 163.6 eV and 164.9 eV are attributed to the spin-split doublet of S $2p_{3/2}$ and S $2p_{1/2}$, respectively.[33] It is important to find that both of the new peaks at higher binding energy, which appear at 166.2 eV and 167.6 eV, are attributed to the sulfur spin-split coupling from C-S^+-C.[27,33] It is concluded that the PEDOT component in the composite films has the oxidized state with the formation of S^+ polaron.

UPS is one of the useful tools for analyzing energy levels involved with π and σ orbits.[34] We measured the UPS spectra of the GO-PEDOT composite films as shown in Fig. 6d. In these UPS spectra, the photoemitted electrons that have the binding energy (BE) lower than 4.9 eV emanated primarily from π orbits, and the electrons with BE higher than 7.3 eV emitted from σ bonds. The electrons with BE in the range from 4.9 eV to 7.3 eV are assigned to orbital overlapping.[34] From Fig. 6d, it can be seen that the π orbits signals in 0~4.9 eV are extraordinary weak for the pure GO. This result is consistent with the fact that the oxidization of GO has turned the sp^2-bonded carbon atoms to be the sp^3-bonded carbon atoms, thus destroying the π bond. In GO-PEDOT composite films, due to the upload of PEDOT, the as-prepared films have a plenty of the delocalized π electrons and exhibit low hole-barrier (Φ_{Hole}) as compared to the pristine GO. The work function of a material can be calculated through the equation:[35]

$$Work\ Function = h\nu - (E_{cutoff} - E_F) \quad (1)$$

where $h\nu$ is the incoming photon energy (21.2 eV) from He I source, E_{cutoff} is the energy cutoff on the high-energy sides, and E_F is the Fermi level. It is calculated from Eq. 1 that the work function is 3.6 eV for GO and 4.8 eV for PEDOT in the composite films, and the hole barrier is 2.8 eV for GO and 0.3 eV for PEDOT component (Fig. 6d). According to the values of the work function and hole barrier, we obtain the energy-level offset between GO and PEDOT components and therefore, we

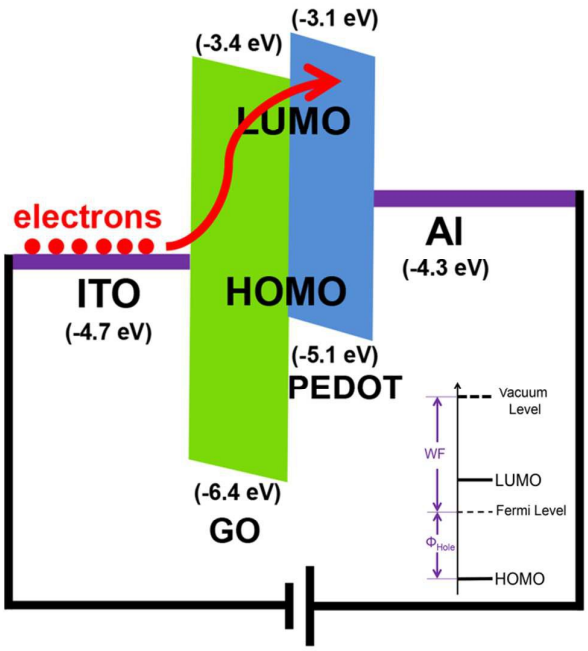

Fig. 7 Schematic diagram of the energy levels for the ITO/GO-PEDOT/Al device. Inset shows the schematic diagram of energy levels. The band gaps of the GO and the PEDOT are taken from Refs.[16,24] The work functions of Al electrode and ITO electrode are taken from Refs.[11,23]

design the ITO/GO-PEDOT/Al film for an organic memory device. The energy levels depicted in Fig. 7 will be used to explore the charge conduction in the organic device.

Resistive switching memory properties

Fig. 8a shows the current-voltage (I-V) characteristics of the ITO/GO-PEDOT/Al device, which is prepared by depositing metal Al on the as-prepared ITO/GO-PEDOT film (See inset in Fig. 8b). As shown in Fig. S1, the thickness of the GO-PEDOT composite films is about 35 nm. The voltage bias is applied to the top Al electrode, and the bottom electrode is grounded. It is observed that the device exhibits the reversible bistable resistance switching between a high resistance state (HRS) and low resistance state (LRS). The first positive sweep yields a high resistance OFF state. When the voltage increases to +1.5 V, an abrupt rise in the current occurs together with the transition from the initial OFF state to the low resistance ON state (Sweep 1). The ON state can be retained after removing the power supply (Sweep 2). In the course of the negative sweep with the reverse voltages being applied to the top Al electrode, the ON state is reset to the OFF state at -3.6 V (Sweep 3). The OFF state of the device can be read (Sweep 4) and reprogrammed to the ON state in the subsequent positive sweep (Sweep 5), thus completing the "write-read-erase-read-rewrite" cycle for a nonvolatile rewritable memory device.[20] It is seen that the two resistance states remain stable even after the voltage is removed, indicating the nonvolatile memory. With the ON/OFF current ratio as high as 3×10^4 at 0.3 V, the reversible resistance switching between HRS and LRS promises to be used in the rewritable data storage system. Furthermore, we have analyzed the retention characteristics of the device

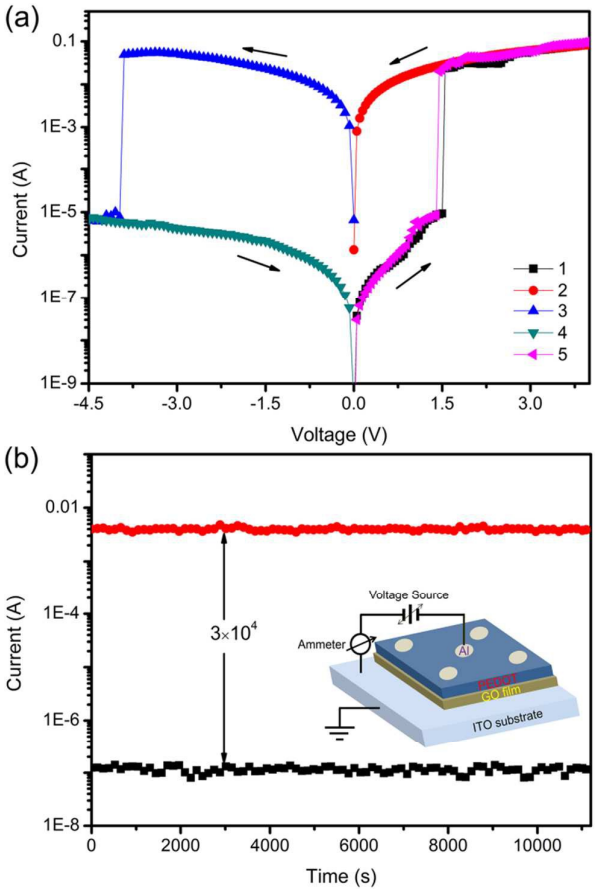

Fig. 8 (a) I-V characteristics of the ITO/GO-PEDOT/Al device. (b) The effect of operation time on the device current in the ON state and OFF state. Inset in (b) represents the schematic diagram of the structure of the ITO/GO-PEDOT/Al device.

for checking the durability. At a constant stress of 0.3 V, no evident decay in the current is detected for both the ON and OFF states over a period of 10^4 s (Fig. 8b).

To elucidate the physical nature of resistance switching effects in the ITO/GO-PEDOT/Al device, the resistances at both LRS and HRS are measured at the temperatures ranging from 294 K to 394 K. As shown in Fig. 9a, the resistance of HRS is found to decrease with increasing temperature, indicating semiconductor property.[10] The temperature dependence of HRS is described by Arhenius law in Eq. (2):[10]

$$R(T) = R_A exp(E_{AC}/kT) \quad (2)$$

where R_A is the Arrhenius pre-exponential factor for resistance, E_{AC} is the activation energy for conduction, k is the Boltzman constant and T is temperature. By fitting the experimental data into Eq. (2), we obtain that E_{AC} is 128 meV.

Fig. 9b shows that as for LRS, the resistance values increase with an increase in temperature. This tendency is typical for electronic transport in metals, implying the presence of metallic conductive paths in LRS.[10,36] The as-observed linear dependence of resistance on temperature is described by the following equation:[36]

$$R(T) = R_0[1 + \alpha(T - T_0)] \quad (3)$$

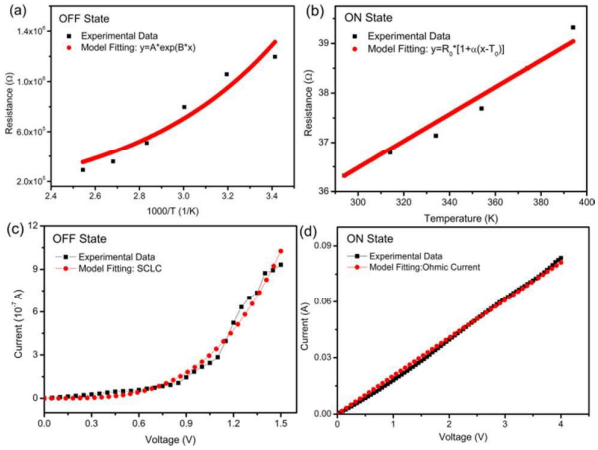

Fig. 9 The temperature dependence of resistances for the ITO/GO-PEDOT/Al device in (a) OFF state and (b) ON state, and the I-V characteristics of the device in (c) OFF state and (d) ON state.

where R_0 is the resistance at temperature T_0, α is the temperature coefficient of resistance, $R(T)$ is the resistance at temperature T. By choosing T_0 as 294 K, the temperature coefficient of resistance of the filaments is calculated to be 7.49×10^{-4} k^{-1}, which is close to the value of bulk Al,[37] confirming that the filaments are composed of Al in metallic states due to the diffusion of the top electrode under a bias voltage. The discrepancy of the temperature coefficient of resistance is attributed to inevitable defects in the Al filaments, since the presence of defects can reduce the temperature coefficient of resistance.

To gain insight into the conductive mechanism of the ITO/GO-PEDOT/Al device, the I-V data are analyzed by using different conduction models which include Ohmic contact, Fowler-Nordheim (F-N) tunneling, space charge limited conduction (SCLC) and thermionic emission limited conduction.[10,35] The results show that the OFF-state can be well described by SCLC model, which is defined as:[35]

$$I = kV^m \quad (4)$$

where I and V is the current and the applied voltage, respectively. The parameter m is related to the density of states of the transport path. The parameter k is associated with the thickness of the film, trap distribution, and the conductivity of the transport path. As shown in Fig. 9c, the model calculation results agree well with the I-V data in the OFF state. Accordingly, the OFF-state charge transport is dominated by SCLC. To synthesize GO, incorporating oxygen functional groups to graphene provides GO with the sp^3-hybridized carbon atoms as the structural defects. The structural defects in GO devote the electron trap to the device.[38] The electron-trapping effect may also resource from the oxidized states in the PEDOT component.[39] In terms of the defect-trapping model, the oxidized state is regarded as a "defect" state for binding electrons.[39] In the course of the first positive sweep, the electrons are forced to transfer from the bottom ITO electrode into the GO-PEDOT film, and the injected electrons are captured and gradually fill in the electron trap nodes. When the trap sites are filled, the conducting paths are erected as a result, the current increases abruptly with the device switching from the OFF state to the ON state. On the other hand, the LUMO level of PEDOT is higher than that of GO, thus forming a barrier in the interface of GO and PEDOT (Fig. 7). In initial HRS with electrons transferring from ITO to Al electrode, the barrier which is built up at the GO-PEDOT interface should decrease the current, enhancing the ON/OFF ratio. As presented in Eq. (5), Ohmic model describes a linear relationship between the current and the applied voltage:[40]

$$I \propto Vexp(-\Delta E_{ae}/kT) \quad (5)$$

where I and V refer to the device current and applied voltage, respectively. ΔE_{ae} is the activation energy of electron. T and k stand for the temperature and Boltzmann constant, respectively. As indicated by the model calculation results in Fig. 9d, the ON-state charge transport is ruled by Ohmic conduction, which is consistent with the metallic conductive behavior in LRS.

It is emphasized here that the previous tests on the I-V characteristics in this study were carried out under ambient condition. We have measured the I-V characteristics of the ITO/GO-PEDOT/Al device under vacuum (See Fig. S2). The results show that the ON/OFF ratio of the device under vacuum is 7×10^3 at 0.3 V and the turn-on voltage is 1 V. Compared with the device under ambient condition, the device under vacuum has less power consumption due to the lower turn-on voltage, meanwhile the ON/OFF ratio changes a little. Moreover, it is found that as compared with the device under vacuum, the device under ambient condition exhibits almost the same ON-state currents and lower OFF-state current, leading to an increase in the ON/OFF ratio. The calculation results in Fig. 9c have revealed that the charge transport at the OFF-state is dominated by SCLC. The lower OFF-state current under ambient condition indicates larger electrical resistance at this condition. It is possible that an insulating Al_2O_3 layer is generated between the Al contact and active layer when the device is tested at air atmosphere and thus, reducing the probability that the charges inject from the Al contact to the active layer.[41]

Several resistance memory devices were fabricated from the composites of PEDOT:PSS and carbon materials, which included rGO,[28] carbon nanoshells[42] and carbon nanotubes.[43,44] These composite materials were prepared by simply mixing the carbon materials with the polymer in solution. As reported, the device using the carbon nanoshells/PEDOT:PSS composite as the active layer showed the write-once-read-many times characteristics instead of the nonvolatile rewritable memory.[42] The rGO/PEDOT:PSS device had the ON/OFF current ratio of about 2 at 0.3 V, meaning unsatisfactory accuracies of programming and erasing.[28] Although the carbon nanotube/PEDOT:PSS device exhibited the ON/OFF current ratio of 10^4 at 0.3 V, the turn-on voltage of the device was as high as 6 V, which meant high power consumption.[44] The GO-PEDOT device of this study exhibits the nonvolatile rewritable memory with the ON/OFF current ratio of 3×10^4 at 0.3 V and turn-on voltage of 1.5 V. With the good performance, the present GO-PEDOT composite memory

device is potentially useful for high capacity and low-cost data storage in future electronics.

Conclusions

In summary, we have presented the nonvolatile rewritable resistance switching properties of the new devices that are fabricated from the GO-PEDOT composite films. These films with the structure of PEDOT growing on GO substrate were prepared through the photochemical polymerization using GO films as the initiators. Having demonstrated by AFM and FESEM-EDX analysis, PEDOT nanoclusters at the size of approximately 50 nm were uniformly generated on the GO films. The work function of the GO and PEDOT components in the composite films had been calculated from the UPS data. TGA and EDX were employed to confirm the content of PEDOT component in GO-PEDOT composites. The PEDOT component was found to have the S^+ polaron as the structure defect. It was measured that the ITO/GO-PEDOT/Al device exhibits a reversible bistable resistance switching with a turn on voltage of 1.5 V, retention capabilities of higher than 10^4 s and the ON/OFF current ratio of 3×10^4. Moreover, the resistance-temperature dependence and model studies obtain that the ON state charge transport in the devices follows Ohmic conduction with a metallic behavior, and the OFF state charge transport is dominated by SCLC with a semiconductor property. This work provides a promising material for the organic RRAM devices.

Acknowledgements

This study was funded by the Science and Technology Commission of Shanghai Municipality (STCSM) under grant no. 13DZ1108904. We are very grateful to Professor Shijin Ding (State Key Laboratory of ASIC and System, School of Microelectronics, Fudan University) for his valuable suggestions and discussions on our work.

Notes and references

1 J. S. Lee, S. Lee and T. W. Noh, *Appl. Phys. Rev.*, 2015, **2**, 031303.
2 J. Park, H. Jeon, H. Kim, W. Jang, H. Seo and H. Jeon, *RSC Adv.*, 2014, **4**, 61064-61067.
3 B. Sun, Y. Liu, W. Zhao and P. Chen, *RSC Adv.*, 2015, **5**, 13513-13518.
4 G. Liu, Y. Chen, R.-W. Li, B. Zhang, E.-T. Kang, C. Wang and X. Zhuang, *ChemElectroChem*, 2014, **1**, 514-519.
5 W.-P. Lin, S.-J. Liu, T. Gong, Q. Zhao and W. Huang, *Adv. Mater.*, 2014, **26**, 570-606.
6 M.-J. Lee, S. Seo, D.-C. Kim, S.-E. Ahn, D. H. Seo, I.-K. Yoo, I.-G. Baek, D.-S. Kim, I.-S. Byun, S.-H. Kim, I.-R. Hwang, J.-S. Kim, S.-H. Jeon and B. H. Park, *Adv. Mater.*, 2007, **19**, 73-76.
7 A. Younis, D. Chu and S. Li, *RSC Adv.*, 2013, **3**, 13422-13428.
8 Q. Zhang, J. Pan, X. Yi, L. Li and S. Shang, *Org. Electron.*, 2012, **13**, 1289-1295.
9 X. Zhuang, Y. Chen, L. Wang, K.-G. Neoh, E.-T. Kang and C. Wang, *Polym. Chem.*, 2014, **5**, 2010-2017.
10 G. Khurana, P. Misra and R. S. Katiyar, *Carbon*, 2014, **76**, 341-347.
11 W. S. Song, H. Y. Yang, C. H. Yoo, D. Y. Yun and T. W. Kim, *Org. Electron.*, 2012, **13**, 2485-2488.
12 Y. Chen, B. Zhang, G. Liu, X. Zhuang and E.-T. Kang, *Chem. Soc. Rev.*, 2012, **41**, 4688-4707.
13 Y. Chen, G. Liu, C. Wang, W. Zhang, R.-W. Li and L. Wang, *Mater. Horiz.*, 2014, **1**, 489-506.
14 X.-D. Zhuang, Y. Chen, G. Liu, P.-P. Li, C.-X. Zhu, E.-T. Kang, K.-G. Neoh, B. Zhang, J.-H. Zhu and Y.-X. Li, *Adv. Mater.*, 2010, **22**, 1731-1735.
15 C. Tan, Z. Liu, W. Huang and H. Zhang, *Chem. Soc. Rev.*, 2015, **44**, 2615-2628.
16 Y. Li, X. Ni and S. Ding, *J Mater Sci. -Mater Electron.*, 2015, **26**, 9001-9009.
17 G. Liu, X. Zhuang, Y. Chen, B, Zhang, J. Zhu, C.-X. Zhu, K.-G. Neoh and E.-T. Kang, *Appl. Phys. Lett.*, 2009, **95**, 253301.
18 S. Porro, E. Accornero, C. F. Pirri and C. Ricciardi, *Carbon*, 2015, **85**, 383-396.
19 B. Zhang, Y.-L. Liu, Y. Chen, K.-G. Neoh, Y.-X. Li, C.-X. Zhu, E.-S. Tok and E.-T. Kang, *Chem. Eur. J.*, 2011, **17**, 10304-10311.
20 G. L. Li, G. Liu, M. Li, D. Wan, K. G. Neoh and E. T. Kang, *J. Phys. Chem. C*, 2010, **114**, 12742-12748.
21 L. Zhang, Y. Li, J. Shi, G. Shi and S. Cao, *Mater. Chem. Phys.*, 2013, **142**, 626-632.
22 Z. Weng, X. Ni, D. Yang, J. Wang and W. Chen, *J. Photochem. Photobiol., A*, 2009, **201**, 151-156.
23 J. Kettle, H. Waters, M. Horie and S.-W. Chang, *J. Phys. D-Appl. Phys.*, 2012, **45**, 125102.
24 S. Lee and K. K. Gleason, *Adv. Funct. Mater.*, 2015, **25**, 85-93.
25 I. Cha, E. J. Lee, H. S. Park, J.-H. Kim, Y. H. Kim and C. Song, *Synth. Met.*, 2014, **195**, 162-166.
26 T. T. Tung, M. Castro, I. Pillin, T. Y. Kim, K. S. Suh and J.-F. Feller, *Carbon*, 2014, **74**, 104-112.
27 J. Zhang and X. S. Zhao, *J. Phys. Chem. C*, 2012, **116**, 5420-5426.
28 S. C. Ray, S. K. Bhunia, A. Saha and N. R. Jana, *Microelectron. Eng.*, 2015, **146**, 48-52.
29 L. Zhang, H. Peng, P. A. Kilmartin, C. Soeller and J. Travas-Sejdic, *Macromolecules*, 2008, **41**, 7671-7678.
30 S.-H. Liao, P.-L. Liu, M.-C. Hsiao, C.-C. Teng, C.-A. Wang, M.-D. Ger and C.-L. Chiang, *Ind. Eng. Chem. Res.*, 2012, **51**, 4573-4581.
31 B. Massoumi, M. Jaymand, R. Samadi and A. A. Entezami, *J. Polym. Res.*, 2014, **21**, 442.
32 B. J. Schultz, R. V. Dennis, J. P. Aldinger, C. Jaye, X. Wang, D. A. Fischer, A. N. Cartwright and S. Banerjee, *RSC Adv.*, 2014, **4**, 634-644.
33 G. Fabregat, B. Teixeira-Dias, L. J. d. Valle, E. Armelin, F. Estrany and C. Alemán, *ACS Appl. Mater. Interfaces*, 2014, **6**, 11940-11954.
34 K. Z. Xing, M. Fahlman, X. W. Chen, O. Inganäs and W. R. Salaneck, *Synth. Met.*, 1997, **89**, 161-165.
35 X. Ma and X. Ni, *Langmuir*, 2014, **30**, 2241-2248.
36 G. Khurana, P. Misra, N. Kumar and R. S. Katiyar, *J. Phys. Chem. C*, 2014, **118**, 21357-21364.
37 Y. Zhang, H. Wu, Y. Bai, A. Chen, Z. Yu, J. Zhang and H. Qian, *Appl. Phys. Lett.*, 2013, **102**, 233502.
38 H. Chang, Z. Sun, M. Saito, Q. Yuan, H. Zhang, J. Li, Z. Wang, T. Fujita. F. Ding, Z. Zheng, F. Yan, H. Wu, M. Chen and Y. Ikuhara, *ACS Nano*, 2013, **7**, 6310-6320.
39 J. Arias-Pardilla, T. F. Otero, R. Blanco and J. L. Segura, *Electrochim. Acta*, 2010, **55**, 1535-1542.
40 Y.-C. Lai, D.-Y. Wang, I-S. Huang, Y.-T. Chen, Y.-H. Hsu, T.-Y. Lin, H.-F, Meng, T.-C. Chang, Y.-J. Yang. C.-C. Chen, F.-C. Hsu and Y.-F. Chen, *J. Mater. Chem. C*, 2013, **1**, 552-559.
41 S. H. Ko, C. H. Yoo and T. W. Kim, *J. Electrochem. Soc.*, 2012, **159**, G93-G96.

42 J. A. Ávila-Niño, E. Segura-Cárdenas, A. O. Sustaita, I. Cruz-Cruz, R. López-Sandoval and M. Reyes-Reyes, *Mater. Sci. Eng., B*, **2011**, 176, 462-466.
43 J. A. Ávila-Niño, W. S. Machado, A. O. Sustaita, E. Segura-Cardenas, M. Reyes-Reyes, R. López-Sandoval and I. A. Hümmelgen, *Org. Electron.*, 2012, **13**, 2582-2588.
44 Y. Sun, L. Li, D. Wen, X. Bai and G. Li, *Phys. Chem. Chem. Phys.*, 2015, **17**, 17150-17158.

Journal Name

ARTICLE

Graphical Abstract

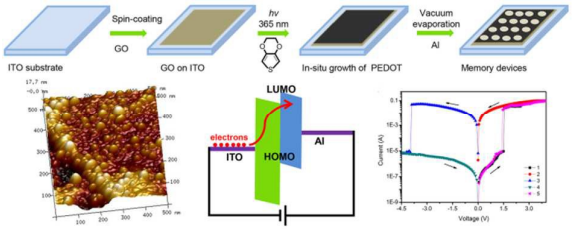

A nonvolatile rewritable memory composite film consisting of PEDOT and GO has been prepared by using GO-initiated photopolymerization.